Generation of radially polarized beams with an image-rotating resonator

Darrell J. Armstrong, Mark C. Phillips, and Arlee V. Smith

We show how a passive image-rotating optical resonator can be used to convert a linearly polarized, lowest-order Gaussian beam into a radially polarized beam. The image and polarization rotation of the cavity removes the frequency degeneracy of the modes, making it possible to select the radially polarized mode by cavity tuning. With the addition of gain, the same cavity should operate as a radially polarized laser when injection seeded at the proper wavelength. © 2003 Optical Society of America

OCIS codes: 230.5750, 140.3410, 140.4780.

1. Introduction

Radially polarized hollow beams are of interest for a variety of applications. For example, radially polarized beams can be used to trap or guide particles that seek the dark beam center,[1,2] to increase the mode volume in a laser cavity,[3,4] for improved laser cutting of metals,[5] for resolution-enhanced microscopy,[6] for probing the orientation of single molecules,[7] and for laser-driven charged particle acceleration.[8,9] Radially and azimuthally polarized modes are modes of cylindrical waveguides and may have low loss in hollow metallic waveguides.[10,11] When a radially polarized beam is focused with high numerical aperture, it produces a strong longitudinal field at the focus.[12] Its strength can exceed the maximum strength of the transverse field. Furthermore, the spot size of the longitudinal field is smaller than the spot size of the ring-mode transverse fields.

Radially polarized beams have been created in a variety of ways, either by manipulating a linearly polarized, lowest-order Gaussian beam or in direct emission from a suitable laser. Tidwell *et al.*[13,14] used interferometric methods to convert filled, linearly polarized beams into radially polarized beams. Other passive methods of generating radially polarized beams include coupling between two laterally offset optical fibers that can preferentially excite radially polarized modes[15] and subwavelength spiral gratings.[16,17]

Radially polarized laser designs include a He–Ne laser with a conical dielectric element that introduces high loss for all but the radially polarized mode.[18] Another design uses an intracavity uniaxial crystal oriented for propagation along the optic axis. The *e*-polarized light refracts more in the crystal than does the *o*-polarized light. If the cavity is designed so that the higher refraction leads to lower loss, the radially polarized mode is favored.[19,20] Maric and Garmire[11] used a hollow metal waveguide as part of the cavity of a CO_2 laser. The lower-loss TM_{0n}, or radially polarized modes, were favored. Concentric-grating surface-emitting lasers have been shown to produce azimuthally polarized beams.[21,22]

In this paper we present another passive method of beam conversion from a linearly polarized filled beam to a radially polarized hollow beam. This conversion is accomplished using a four-mirror image-rotating optical resonator. We anticipate that the same resonator should prove capable of generating radially polarized beams directly as a laser.

Figure 1 shows a radially polarized mode along with the closely related azimuthally polarized and hybrid modes. Each has a dark center because light on opposite sides of the beam are phase reversed. The half-wave retarders shown in Fig. 1 convert among the modes. For example, the azimuthally polarized mode can be converted into the radially polarized mode using two half-wave retarders oriented 45° apart. All three of these modes propagate without change in character, meaning that, although their radial profiles may change, they each retain their dark center and polarization distributions.

The authors are with Sandia National Laboratories, Department 1118, Albuquerque, New Mexico 87185-1423. The e-mail address for A. V. Smith is arlsmit@sandia.gov.

Received 16 January 2003; revised manuscript received 19 March 2003.

0003-6935/03/183550-05$15.00/0

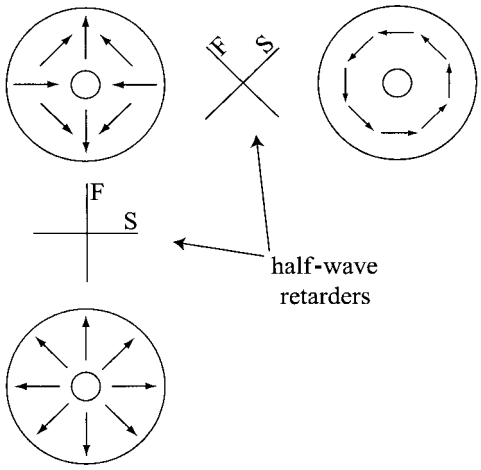

Fig. 1. Three cylindrically polarized modes: azimuthally polarized (upper right), radially polarized (lower left), hybrid polarized (upper left). The half-wave retarders, oriented as shown, convert between the adjacent polarization modes.

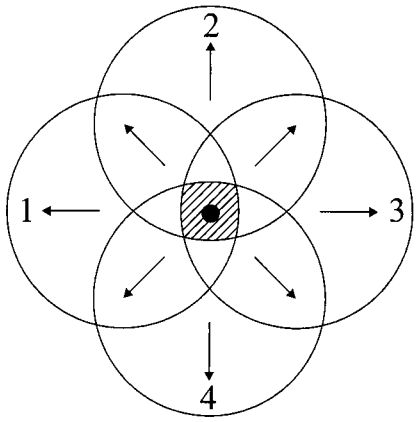

Fig. 3. Beams from cavity passes 1, 2, 3, and 4 as seen at the exit mirror M_2. The input beam is offset from the cavity axis, which is indicated by the center dot. The cavity rotates both the beam position and the polarization angle by 90°. The cavity length is adjusted to give the phases as shown, resulting in a radially polarized beam. If the input polarization is rotated by 90°, the beam is azimuthally polarized. If the cavity length is changed by $\lambda/2$, the mode is hybrid polarized, as shown in Fig. 1.

2. Experiment

Our resonator, shown in Fig. 2, was described in detail in an earlier paper.[23] Briefly, it is a nonplanar four-mirror ring with two long legs, L_1 and L_3, and two short legs, L_2 and L_4, with a $\sqrt{2}$ length ratio of the long to short sides. This ratio, combined with the orthogonal planes of reflection at mirrors M_1 and M_2, gives a 90° rotation of the beam on each round trip of the cavity. Like all image-rotating cavities, it has a unique optical axis. Only rays that coincide with the axis retrace themselves on each cavity pass. Rays parallel to the axis but displaced laterally will retrace after four cavity passes. If all the cavity mirrors have equal reflectivities for the s and p polarizations, the polarization will also be rotated by 90° on each cavity pass. Note that if the input beam is s or p polarized relative to M_2, then the polarization will also be rotated by 90°, even if there are differences in the reflectivities for s and p polarizations.

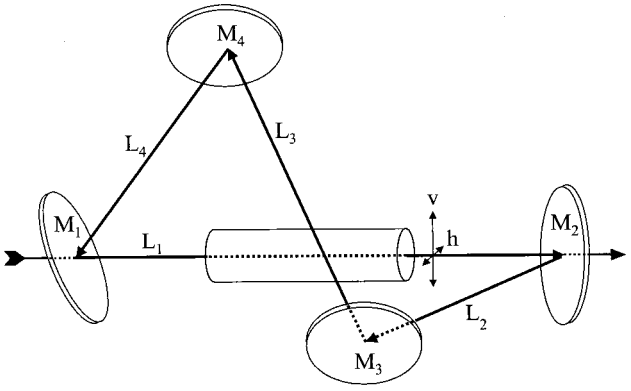

Fig. 2. Image-rotating optical cavity. Light enters through mirror M_1 and exits through mirror M_2. The reflection plane at M_2 is horizontal (h), the reflection plane at M_1 is vertical (v). With the leg lengths $L_1 = L_3 = \sqrt{2}L_2 = \sqrt{2}L_4$, the cavity produces a 90° image rotation on each round trip. The cylinder is an optional, isotropic gain medium.

Figure 3 shows how a radially polarized mode can be excited by illuminating mirror M_1 with a linearly polarized beam that is offset but parallel to the cavity axis. The incident beam is labeled 1. After one pass of the cavity the position will be rotated 90° about the cavity axis, and the resulting beam is labeled 2. As noted above, the polarization will be rotated by 90° if all mirrors reflect s- and p-polarized light identically or if the incident beam is s or p polarized. Subsequent passes around the cavity give the beams labeled 3 and 4. If the cavity length is adjusted so the phase of the beams on opposite sides of the axis are 180° out of phase, the beam center will be dark. There are then two possibilities for the phase of beam 2. It can be +90° or −90° phase shifted relative to beam 1, assuming there is no phase shift between s- and p-polarized waves. In either case the cavity will be resonant, but one case gives a radially polarized beam whereas the other gives the hybrid polarization of Fig. 1.

For our experimental studies, we used four identical dielectric mirrors with reflectivities of 0.95 and 0.87 for s and p polarizations, respectively, and with a measured s-to-p phase shift of less than 4°. A zeroth-order Gaussian beam from a single-mode Ti: sapphire laser (λ = 800 nm) was input into the cavity through mirror M_1 at a horizontal offset from the cavity axis. To excite radial and hybrid modes, the polarization of the input beam was set to be horizontal. Figure 4 shows an irradiance profile of a hollow beam emerging from mirror M_2, measured with a CCD camera. We determined the polarization properties of the modes by placing a linear polarizer in the emerging beam. Figure 5 shows sample irradiance profiles of the analyzed radial and hybrid modes. In

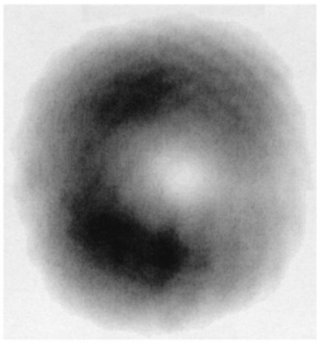

Fig. 4. Measured irradiance profile of a radially polarized hollow beam.

the radially polarized case the transmitted two-lobed irradiance pattern rotated in the same direction as the polarizer, whereas for the hybrid mode the pattern rotated in the opposite direction from the polarizer. These behaviors are consistent with the polarizations of the modes shown in Fig. 1.

The radially polarized and hybrid polarized modes are not frequency degenerate. The cavity length must be changed by $\lambda/2$ to change the output from one mode to the other. We experimentally switched between the modes by tuning the wavelength of the input laser. We also note that an azimuthally polarized beam could be generated for the same cavity length as the radially polarized beam by rotating the polarization of the injected beam by 90°.

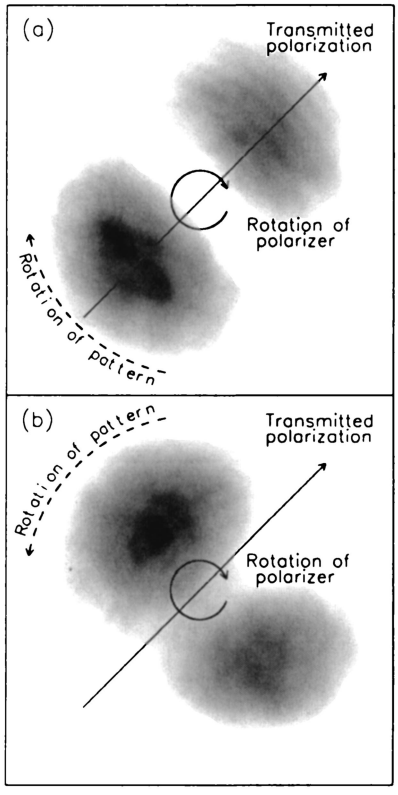

Fig. 5. Measured irradiance profiles after passing through a linear polarizer. (a) Pattern for a radially polarized beam. When the polarizer was rotated, the pattern rotated in the same direction as the polarizer. (b) Pattern for a hybrid polarized beam. When the polarizer was rotated, the pattern rotated in the opposite direction as the polarizer.

3. Cavity-Mode Description

It is instructive to describe the cavity in terms of its eigenpolarizations. In this analysis we ignore diffraction because the beam diameters are large and the mirrors are planar. The positioning of the beams after traversing the cavity is determined entirely by the image-rotating property of the cavity that in turn is determined solely by the cavity geometry. The polarization behavior, in contrast, depends also on the mirror reflectivities. We can analyze the polarization evolution using standard matrix methods. From the cavity geometry we know[23] that the plane of incidence for mirror M_3 is rotated by 45° from that at mirror M_2. Similarly the planes for mirrors M_1 and M_4 lie 45° apart. The planes of incidence rotate by 90° in going from mirror M_1 to mirror M_2 and in going from mirror M_3 to M_4. Starting at the cylinder in Fig. 2 and proceeding around the cavity, we reflect from M_2, rotate by 45°, reflect from M_3, rotate by 90°, reflect from M_4, rotate by 45°, reflect from M_4, and rotate by 90°. This puts us back in the original reference frame. Describing the optical field as

$$E = E_0 \begin{bmatrix} v \\ h \end{bmatrix}, \tag{1}$$

the round trip is described by

$$M_{\text{roundtrip}} = M_{\text{rot},90} M_{\text{ref},1} M_{\text{rot},45} M_{\text{ref},4} \times M_{\text{rot},90} M_{\text{ref},3} M_{\text{rot},45} M_{\text{ref},2}, \tag{2}$$

where $M_{\text{ref},i}$ is the matrix that describes the transformation of the polarization on reflection from mirror M_i,

$$M_{\text{ref},i} = \begin{bmatrix} r_{si} & 0 \\ 0 & r_{pi} \exp(i\phi_i) \end{bmatrix}, \tag{3}$$

with r_{si} being the amplitude of the reflection coefficient for s-polarized light at mirror M_i, r_{pi} being the amplitude of the reflection coefficient for p-polarized light, and ϕ_i being the phase shift between the p and s reflection coefficients. $M_{\text{rot},45}$ is the matrix for 45° rotation:

$$M_{\text{rot},45} = \frac{1}{\sqrt{2}} \begin{bmatrix} 1 & 1 \\ -1 & 1 \end{bmatrix}. \tag{4}$$

If mirrors M_3 and M_4 are identical, ($\phi_3 = \phi_4 \equiv \phi$), ($r_{s,3} = r_{s,4} \equiv r_s$), ($r_{p,3} = r_{p,4} \equiv r_p$), and the section of the round-trip matrix describing their reflections is

$$(M_{\text{ref},4} M_{\text{rot},90} M_{\text{ref},3}) = r_s r_p \exp(i\phi) \begin{bmatrix} 0 & 1 \\ -1 & 0 \end{bmatrix}, \tag{5}$$

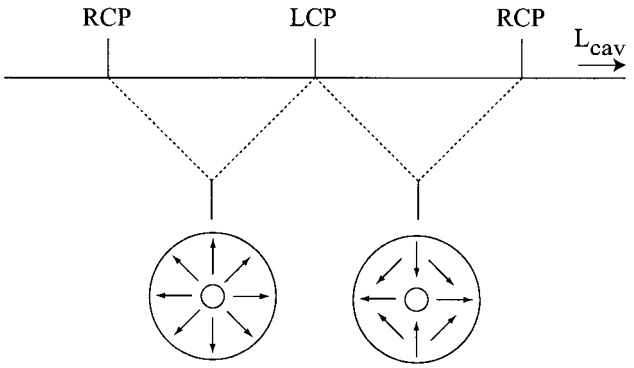

Fig. 6. Resonances versus cavity length. The right- and left-circularly polarized resonances are offset by $\lambda/2$ and support the filled beams. Tuned midway between the LCP and the RCP resonances, the cavity supports vortex modes of each polarization but with opposite vorticities or charges. One combination of vortex modes is the radially polarized beam, the other is the hybrid polarized beam.

which is equivalent to a 90° rotation accompanied by an overall reflectivity of $r_s r_p$ and a phase shift of ϕ. The full round-trip matrix is

$$M_{\text{roundtrip}} = r_s r_p \exp(i\phi) \times \begin{bmatrix} 0 & -r_{p2} r_{p1} \exp(i\phi_1 + i\phi_2) \\ r_{s1} r_{s2} & 0 \end{bmatrix}. \quad (6)$$

To simplify the calculation of the eigenmodes for a single round trip of the cavity, we make some assumptions about the mirrors. In our measurements we used four identical mirrors that have reflectivities of 0.95 for s polarization and 0.87 for p polarization. We assume that the s-to-p phase shift is zero, so our round-trip matrix becomes

$$M_{\text{roundtrip}} = 0.91 \begin{bmatrix} 0 & -0.87 \\ 0.95 & 0 \end{bmatrix}, \quad (7)$$

which we approximate for simplicity as

$$M_{\text{roundtrip}} = 0.83 \begin{bmatrix} 0 & -1 \\ 1 & 0 \end{bmatrix}. \quad (8)$$

For a single pass of the cavity, the eigenpolarizations are $(1, i)$ and $(1, -i)$, or right-circular polarization (RCP) and left-circular polarization (LCP). Calculating the eigenvalues for the two circular polarizations indicates that a round-trip pass of the cavity introduces a phase shift of $\pm 90°$. These phase shifts are expected from the polarization rotation caused by the cavity. Because the cavity rotates the polarization by 90°, this will either advance or retard the phase of a circularly polarized beam by 90° depending on whether it is right- or left-circularly polarized.

The differing phase shifts split the resonances of LCP and RCP light, as shown in Fig. 6, with a cavity length difference of $\lambda/2$ between the two resonances. If we tune to a RCP resonance and displace the incident circularly polarized beam from the axis, the mode looks like that in Fig. 7(a). It is a filled beam because there is no phase reversal on opposite sides of the beam. If we then lengthen the cavity by $\lambda/4$, each cavity pass introduces an additional 90° phase shift, and the mode becomes that of Fig. 7(b). In the language sometimes used to describe beams with a helical phase front, this is a circularly polarized charge (+1) vortex or doughnut mode[1,24] where the magnitude of the charge is the number of waves of phase advance around the dark center of the beam and the sign indicates the direction of the phase ramp. This beam has a net angular momentum of zero because the spin and orbital angular momentums cancel one another.[25] Degenerate with this mode is a charge (−1) vortex mode of LCP. Added coherently, these two modes are the radially polarized beam shown in Fig. 6. Lengthening the cavity by $\lambda/2$ tunes to a pair of degenerate vortex modes with reversed charges, and the sum of those is the hybrid mode shown in Fig. 6.

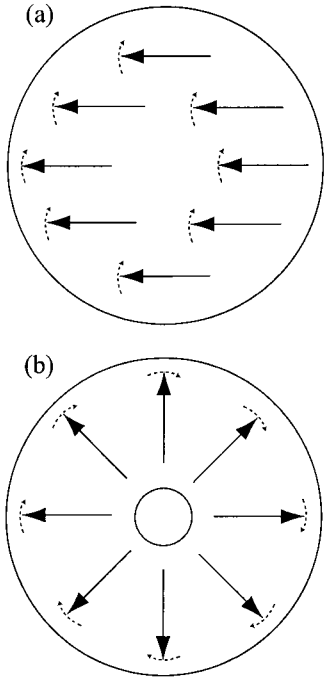

Fig. 7. (a) Schematic of the polarization distribution when the incident light is circularly polarized and the cavity is tuned to resonance. The beam is filled in because there is no phase reversal on opposite sides of the beam. (b) Schematic of the polarization distribution when the cavity is lengthened by $\lambda/4$ to produce a circularly polarized vortex beam.

4. Conclusions

We have demonstrated that using a cavity with 90° image rotation on each pass breaks the frequency degeneracy of vortex modes of different charge. With appropriate seeding this allows us to reliably and efficiently generate high-quality vortex modes. By controlling the polarization and wavelength of the beam input into the passive cavity, we were able to produce radially polarized hollow beams. We antic-

ipate that placing an isotropic gain medium such as Nd:glass in the cavity will produce similar behavior if the lasing frequency is determined by seed light tuned to one of the cavity resonances. For the gain of the ring modes to compete with the filled beam modes it may be necessary to have an annular gain profile that matches the ring mode. If the gain medium has thermally induced birefringence with a radial distribution, as is commonly the case, the azimuthally and radially polarized modes should shift apart in frequency, so it may be possible to preferentially excite one or the other by frequency selection.

Sandia is a multiprogram laboratory operated by Sandia Corporation, a Lockheed Martin Company, for the U.S. Department of Energy's National Nuclear Security Administration under contract DE-AC04-94AL85000.

References

1. K. T. Gahagan and G. A. Swartzlander, Jr., "Simultaneous trapping of low-index and high-index microparticles observed with an optical-vortex trap," J. Opt. Soc. Am. B **16,** 533–537 (1999).
2. T. Kuga, Y. Torii, N. Shiokawa, T. Hirano, Y. Shimizu, and H. Sasada, "Novel optical trap of atoms with a doughnut beam," Phys. Rev. Lett. **78,** 4713–4716 (1997).
3. E. Abramochkin, N. Losevsky, and V. Volostnikov, "Generation of spiral-type laser beams," Opt. Commun. **141,** 59–64 (1997).
4. R. Oron, N. Davidson, A. A. Friesem, and E. Hasman, "Efficient formation of pure helical laser beams," Opt. Commun. **182,** 205–208 (2000).
5. V. G. Niziev and A. V. Nesterov, "Influence of beam polarization on laser cutting efficiency," J. Phys. D **32,** 1455–1461 (1999).
6. S. Quabis, R. Dorn, M. Eberler, O. Glockl, and G. Leuchs, "Focusing light to a tighter spot," Opt. Commun. **179,** 1–7 (2000).
7. L. Novotny, M. R. Beversluis, K. S. Youngworth, and T. G. Brown, "Longitudinal field modes probed by single molecules," Phys. Rev. Lett. **86,** 5251–5254 (2001).
8. L. P. Campbell, C. E. Dilley, S. C. Gottschalk, W. D. Kimura, D. C. Quimby, L. C. Steinhauer, M. Babzien, I. Ben-Zvi, J. C. Gallardo, K. P. Kusche, Jr., I. V. Pogorelsky, J. R. Skaritka, A. van Steenbergen, V. E. Yakimenko, D. B. Cline, P. He, Y. Liu, and R. H. Pantell, "Inverse Cerenkov acceleration and inverse free-electron laser experimental results for staged electron laser acceleration," IEEE Trans. Plasma Sci. **28,** 1094–1102 (2000).
9. C. Varin and M. Piche, "Acceleration of ultra-relativistic electrons using high-intensity TM_{01} laser beams," Appl. Phys. B **74,** S83–S88 (2002).
10. A. A. Tovar, "Production and propagation of cylindrically polarized Laguerre–Gaussian laser beams," J. Opt. Soc. Am. A **15,** 2705–2711 (1998).
11. M. E. Maric and E. Garmire, "Low-order TE_{0q} operation of a CO_2 laser for transmission through circular metallic waveguides," Appl. Phys. Lett. **38,** 743–745 (1981).
12. K. S. Youngworth and T. G. Brown, "Focusing of high numerical aperture cylindrical-vector beams," Opt. Exp. **7,** 77–87 (2000), http://www.opticsexpress.org.
13. S. C. Tidwell, G. H. Kim, and W. D. Kimura, "Efficient radially polarized laser beam generation with a double interferometer," Appl. Opt. **32,** 5222–5229 (1993).
14. S. C. Tidwell, D. H. Ford, and W. D. Kimura, "Generating radially polarized beams interferometrically," Appl. Opt. **29,** 2234–2239 (1990).
15. T. Grosjean, D. Courjon, and M. Spajer, "An all-fiber device for generating radially and other polarized light beams," Opt. Commun. **203,** 1–5 (2002).
16. Z. Bomzon, V. Kleiner, and E. Hasman, "Formation of radially and azimuthally polarized light using space-variant subwavelength metal stripe gratings," Appl. Phys. Lett. **79,** 1587–1589 (2001).
17. Z. Bomzon, G. Biener, V. Kleiner, and E. Hasman, "Radially and azimuthally polarized beams generated by space-variant dielectric subwavelength gratings," Opt. Lett. **27,** 285–287 (2002).
18. Y. Mushiake, K. Matsumura, and N. Nakajima, "Generation of radially polarized optical beam mode by laser oscillation," Proc. IEEE **60,** 1107–1109 (1972).
19. J. J. Wynne, "Generation of the rotationally symmetric TE_{01} and TM_{01} modes from a wavelength-tunable laser," IEEE J. Quantum Electron. **QE-10,** 125–127 (1974).
20. D. Pohl, "Operation of a ruby laser in the purely transverse electric mode TE_{01}," Appl. Phys. Lett. **20,** 266–267 (1972).
21. A. A. Tovar and G. H. Clark, "Concentric-circle-grating, surface-emitting laser beam propagation in complex optical systems," J. Opt. Soc. Am. A **14,** 3333–3340 (1997).
22. R. H. Jordan, D. G. Hall, O. King, G. Wicks, and S. Rishton, "Lasing behavior of circular grating surface-emitting semiconductor lasers," J. Opt. Soc. Am. B **14,** 449–453 (1997).
23. A. V. Smith and D. J. Armstrong, "Nanosecond optical parametric oscillator with 90° image rotation: design and performance," J. Opt. Soc. Am. B. **19,** 1801–1814 (2002).
24. D. Ganic, X. Gan, M. Gu, M. Hain, S. Somalingham, S. Stankovic, and T. Tschudi, "Generation of doughnut laser beams by use of a liquid-crystal cell with a conversion efficiency near 100%," Opt. Lett. **27,** 1351–1353 (2002).
25. S. M. Barnett, "Optical angular-momentum flux," J. Opt. B: Quantum Semiclassical Opt. **4,** S1–S10 (2002).